

# Methane conversion via photocatalytic reactions

Charles E. Taylor\*

US Department of Energy, National Energy Technology Laboratory, P.O. Box 10940, Pittsburgh, PA 15236-0940, USA

## Abstract

Research on the conversion of natural gas (methane) has been an ongoing effort at the National Energy Technology Laboratory (NETL) for over 20 years. A long-term goal of our research team is to explore novel pathways for the direct conversion of methane to liquid fuels, chemicals, and intermediates. One of our current areas of research is the conversion of methane to methanol, under mild conditions, using light, water, and a semiconductor photocatalyst. The use of three relatively abundant and inexpensive reactants—light, water, and methane—to produce methanol is an attractive process option. The main advantage of using a photocatalyst to promote the photoconversion of methane to methanol is that the presence of the catalyst, in conjunction with an electron-transfer agent, allows reaction to occur with visible light instead of with ultraviolet. This greatly simplifies reactor design and will permit flexibility in the selection of the light source. The products of the reaction of interest, methanol and hydrogen, are both commercially desirable as fuels or chemical intermediates. Reactions were conducted at 1.0 and 10.1 MPa along with methane contained within gas hydrates.

Published by Elsevier B.V.

**Keywords:** Methane; Methanol; Tungsten oxide; Photocatalytic

## 1. Introduction

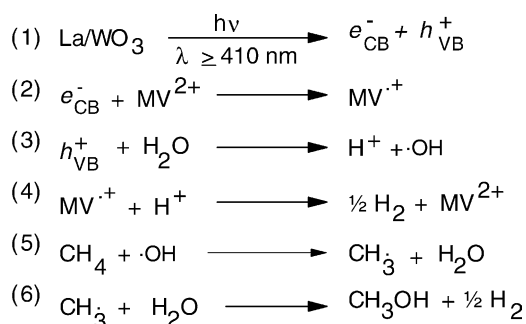
A global research effort is underway in academia, industry, and government to find methods to convert methane to useful, more readily transportable and storable materials. Methanol, the initial product of methane oxidation, is a desirable product of conversion because it retains much of the original energy of the methane while satisfying transportation and storage requirements. A liquid at room temperature, methanol could be transported to market using the existing petroleum pipeline and tanker network and distribution infrastructure. Publications have indicated that photochemical oxidation of methane may be a commercially feasible route to methanol [1–5]. Research in our laboratory [6–8] has shown that methane,

dissolved in water, at temperatures  $>373$  K, in the presence of a semiconductor catalyst and electron-transfer agent, can be converted to methanol and hydrogen. The chemistry is described by Eqs. (1)–(6) [3]. Conversion of methane is limited by the quantity of methane that can be dissolved in the water. We hypothesized that if the concentration of methane in water can be increased, conversion should also increase.

This can be accomplished by increasing the head-space pressure of methane or by the use of methane hydrates. Methane hydrates are clathrates that are in the form of a methane–water ice-like crystalline material, is stable, and occurs naturally in deep-ocean and permafrost areas (Fig. 1 [9]). Methane hydrates form in the ocean at depths between  $\sim 280$  and 4000 m, water temperatures between 273 K (at 280 m) and 296 K (at 4000 m), and water pressure between 4.14 MPa at 280 m to 41.4 MPa at 4000 m. In cold polar regions, two parallel events occur: (1) surface temperatures

\* Tel.: +1-412-386-6058; fax: +1-412-386-4806.

E-mail address: charles.taylor@netl.doe.gov (C.E. Taylor).



$e_{\text{CB}}^-$  = electron in conduction band,  $h_{\text{VB}}^+$  = positive hole in valance band

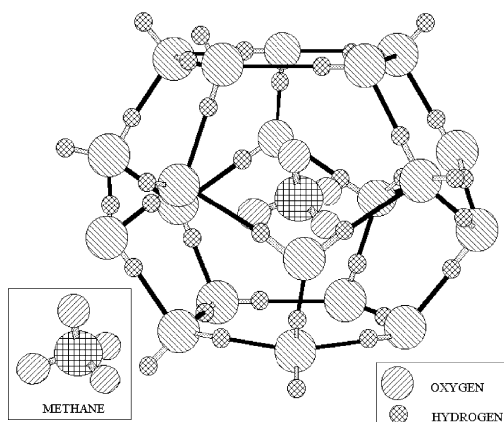


Fig. 1. Schematic of methane hydrate structure I [6].

hovering around 283 K, even with a normal geothermal gradient, generate sub-freezing temperatures that can persist to depths of 600 m or more and (2) the very low temperatures, when combined with steadily increasing subsurface pressures, allow the formation of methane hydrate and allow it to be stable at depths ranging from 300 m to 1 km. At standard temperature and pressure (STP) one volume of saturated methane hydrates contains approximately 180 volumes of methane. Thus, the conditions that are favorable for the formation of permafrost are also the conditions that are favorable for gas hydrates to form. Current estimates suggest that there is twice as much organic carbon contained in methane hydrates than all other forms of fossil fuels combined.

Another interesting aspect of methane hydrates is the close proximity of the methane to the water molecules. In an ideal methane hydrate molecule, there are 5.75 water molecules for each methane molecule,

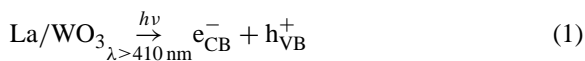
a much higher methane concentration (15 mol% methane) than can be obtained by pressurizing a reactor containing water and methane. As shown in Eq. (3), the reaction involves the formation of hydroxyl radical ( $\cdot\text{OH}$ ) from water by photochemical means. The proximity and restricted mobility of  $\cdot\text{OH}$  and  $\text{CH}_4$  would then favor the formation of  $\text{CH}_3\text{OH}$  in methane hydrates. We have demonstrated in our laboratory [10] that methane within the hydrate lattice can be converted to methanol and hydrogen when illuminated with light.

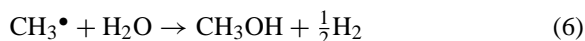
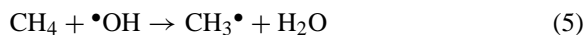
## 2. Experimental

The tungsten oxide semiconductor photocatalysts were synthesized following a modification of the procedure in the literature [4]. Four dopants, copper, lanthanum, platinum, and a mixture of copper and lanthanum, were selected for study on the tungsten oxide catalyst base. The titania photocatalyst used in this study is a proprietary sol-gel  $\text{TiO}_2$  catalyst obtained from Attia Corporation.

The 1.0 MPa, a commercially supplied 1 l quartz photochemical reaction vessel, was fitted to meet the needs of this research. This included use of a Teflon<sup>®</sup>-coated magnetic stirring bar in the reactor, a fritted glass sparger, a nitrogen line used to cool the UV lamp, and an injection port.

In a typical 1.00 MPa pressure experiment, the sintered catalyst is suspended, by mechanical stirring, in double-distilled water ( $\sim 750$  ml) containing an electron-transfer reagent, methyl viologen dichloride. A mixture of methane (5 ml/min) and helium (16 ml/min) is sparged through the photocatalytic reactor. The helium is an internal standard for on-line analysis of the reactor effluent. The reaction temperature is maintained at  $\sim 371$  K by circulation of heated ( $\sim 393$  K) silicone oil in the outer jacket of the reactor. A high-pressure mercury-vapor quartz lamp is used as the light source:





All reactions above 1.0 MPa were conducted in a high-pressure view cell. The cell, constructed of 316 stainless steel, is 6.35 cm (2.5 in.) OD and 27.4 cm (11 in.) in length, with an internal volume of ~40 ml. The cell is fitted with two machined endcaps, one, which contains a sapphire window. The other end of the cell is fitted with an endcap. A fill port, a pressure transducer, and a thermocouple that terminates inside the cavity of the cell are attached axially at a location approximately 10 cm (4 in.) from the sapphire window. While the working pressure of the cell is rated at 220 MPa (32 000 psia), all experiments were conducted at 13.8 MPa (2000 psig) or less. Temperature is controlled by an external circulating temperature bath. The glycol/water solution in the bath is circulated through a 0.64 cm (1/4 in.) copper tubing coiled around the outside of the cell. Several layers of insulating material are wrapped around the cell to help maintain constant temperature. In all experiments, the contents of the cell are mechanically stirred by means of a Teflon<sup>®</sup>-coated magnetic stir bar. An external magnetic stirrer is used to power the stir bar.

A typical experiment for the pressurized photocatalytic conversion of methane and water reaction begins by filling the high-pressure cell with 10 ml of double-distilled water. A Teflon<sup>®</sup>-coated stir bar is added followed by the photocatalyst and electron-transfer reagent. An external magnetic stirrer is used to obtain a high degree of vortex mixing inside the cell. The cell is connected to the gas manifold and purged several times with methane. The cell is charged with methane 10.1 MPa (1470 psig) and isolated from the manifold by two valves. Temperature of the water in the cell is increased to 50 °C and held constant. Illumination of the hydrate is performed by the use of a high-pressure 350 W mercury-vapor lamp. After illumination for a set period of time, the contents of the cell are vented.

A typical experiment for conversion of methane hydrates is similar to the >1 MPa experiments. After purging several times with methane, the cell is charged with methane 5.5–13.8 MPa (800–2000 psig) and isolated from the manifold by two valves. Temperature of the water in the cell is lowered until formation of the methane hydrate is observed. After

formation of the hydrate, the temperature of the cell is lowered to 268 K and held constant. Illumination of the hydrate is performed by the use of a high-pressure 350 W mercury-vapor lamp. After illumination for a set period of time, the cell is allowed to warm slowly to room temperature. When the cell and its contents have reached room temperature, the contents of the cell are vented.

The gaseous products of all reactions are analyzed on-line and in real time by a quadrupole mass spectrometer.

Four doped tungsten oxide catalysts (noted above) were synthesized and used in this study. The catalysts were analyzed by scanning electron microscopy (SEM), energy dispersive X-ray spectroscopy (EDS), X-ray diffraction (XRD), and X-ray photoelectron spectroscopy (XPS). For all catalysts, except the platinum-doped tungsten oxide, these techniques were not able to detect any differences between the tungsten oxide, as received, and the unsintered-doped oxide. This is due to the level of doping, 4 at.%, which is below the detection limits of these instruments. The sintering process produced differences that were detectable by SEM and XRD. After sintering, XRD data showed the doped tungsten oxides to be more crystalline than the unsintered materials as evidenced by the separation of a broad diffraction peak into two separate peaks having  $2\theta$  values of 28.8° and 42.0°. Analysis of the sintered, doped tungsten oxides by SEM revealed that the sintered materials contained larger crystallites with smoother edges. The catalysts were each tested for their ability to catalytically photolyze water prior to their use in the methane conversion experiments.

### 3. Results

Of the four-tungsten oxide (doped with platinum, lanthanum, copper, and a 50/50 molar mixture of copper and lanthanum) and the sol–gel titania catalysts studied, the tungsten oxide catalyst doped with lanthanum exhibited the largest methane conversion and methanol yield. This catalyst was the one chosen for use in this study.

Fig. 2 shows the results of a typical photocatalytic methane conversion experiment at 1.0 MPa. Methane conversions are ~4% with hydrogen and methanol as

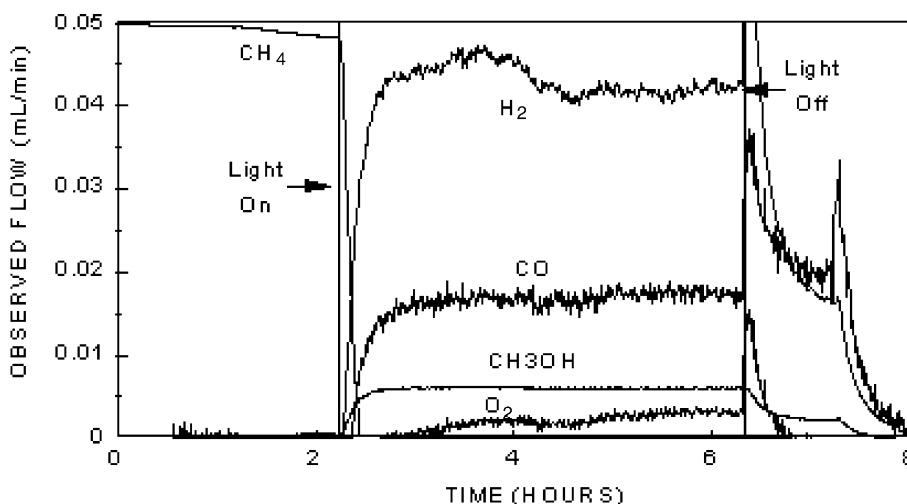


Fig. 2. Products of the photocatalytic conversion of methane in water at 1.00 MPa and 370 K.

the main products of reaction. Note that after the UV lamp is turned off, the detected flow of methanol decreases slowly to zero (over ~2 h). It was hypothesized that this behavior was due to stripping of methanol from the water in the reactor by the reactant gases. To confirm this, methanol was injected into the reactor, previously filled with 750 ml water at the operating temperature, and the concentration of methanol in the gas flow from the reactor was measured as a function of time. A decrease in methanol concentration over several hours, similar to that observed in experiments undergoing methane photoconversion, was observed.

As noted previously, the proposed reaction sequence of interest initially produces hydroxyl radical, which then reacts with methane to produce methanol. To test the validity of this hypothesis, a 30% solution of hydrogen peroxide, a good source of hydroxyl radicals, was injected into the reactor during photocatalytic methane conversion. After peroxide injection, conversion of methane increases from ~4% to ~10%, methanol production increases 17-fold, and carbon dioxide increases 5-fold, along with modest increases in hydrogen and carbon monoxide. A drop in methane conversion to zero for approximately 12 min after injection of the hydrogen peroxide solution was observed in all experiments. This drop in methane conversion can be explained by assuming that prior to injecting hydrogen peroxide solution, a steady-state condition existed between the methane dissolving in

the water and methane being consumed. It is likely that the introduction of excess hydroxyl radicals depleted the dissolved methane. At the temperature where the reactions were conducted, the solubility of methane in water is very low (0.017 ml of methane per milliliter of water [11]). This low solubility results in little methane available for conversion until steady-state conditions could be re-established.

Note that in Fig. 2, after the UV lamp is turned off, the detected flow of methanol decreases slowly to zero (over ~2 h). This is due to stripping of dissolved methanol from the water in the reactor by the reactant gases. Gas chromatographic analysis of the liquid product that had condensed in the trap at 273 K revealed the presence of methanol and acetic acid. Further analysis to identify other components by GC-MS was not possible due to the low concentration of products in the trap. The products were diluted by water carried over from the reactor in the flow of helium that is used as an internal standard.

The tungsten oxide photocatalyst is reported to function at wavelengths >410 nm (Fig. 3). All results reported above were obtained using the UV lamp's total spectrum output. In order to separate reactions initiated by radiation with UV light from reactions initiated by visible light, a filter was constructed to block the UV portion of the lamp's energy output. The filter, a Pyrex® sleeve fitted around the lamp, absorbs nearly all radiation below ~310 nm. The total energy

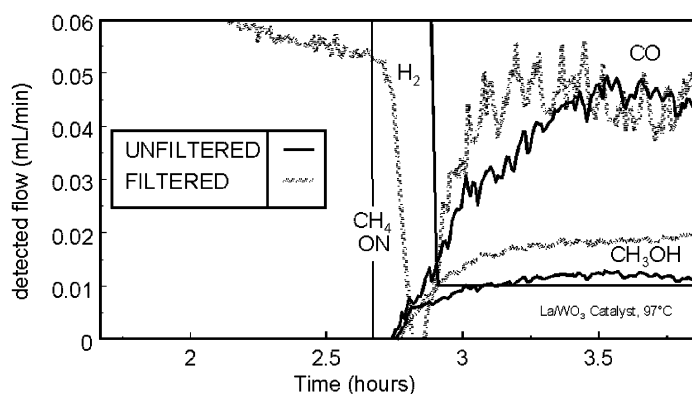


Fig. 3. Products of the photocatalytic reaction of methane dissolved in water at atmospheric pressure and 97 °C with full spectrum and filtered (visible) light.

output of the lamp with the filter in-stalled is  $\sim 50\%$  of that without the filter. Experiments using the filter around the lamp were conducted under conditions described above. The results of experiments conducted with the UV filter installed gave similar conversions and product selectivities as those observed using the full spectrum of the lamp (Fig. 4).

Photocatalytic conversion of methane and water at 10.1 MPa produced a product slate similar to that obtained at atmospheric pressure. What is of note is that while no conversion of methane was observed for the experiments conducted at atmospheric pressure at temperatures less than 343 K, at 10.1 MPa conversion occurred at 323 K.

The majority of the photocatalytic research, including the photocatalytic conversion of methane in methane hydrates, was performed with the lanthanum-

promoted tungsten oxide photocatalyst. Fig. 4 shows the results of photocatalytic conversion of methane dissolved in water at atmospheric pressure and 97 °C for various dopants. As is shown, the catalyst doped with lanthanum out performs the other doped catalyst for the production of methanol.

Photocatalytic conversion of the methane contained within the methane hydrate molecule produced results similar to the two previously described experiments; methanol and hydrogen were the main products. This is an interesting result as at atmospheric pressure, no photocatalytic conversion of methane dissolved in water is observed at temperatures below 70 °C. The photocatalytic conversions of the methane hydrate occurred at temperatures of  $-5^{\circ}\text{C}$  and below.

Analysis, by mass spectrometry (Fig. 5), of the gas contained in the headspace of the cell after

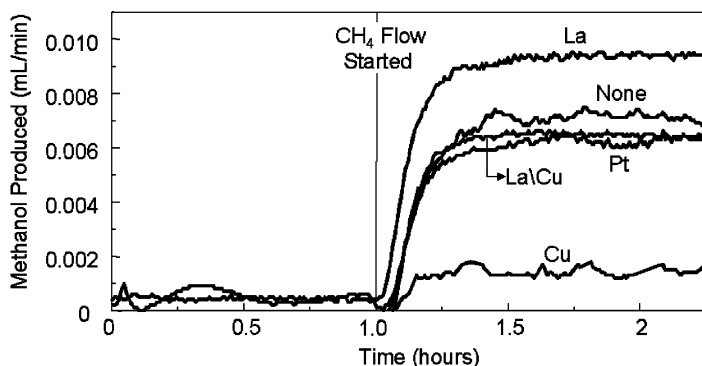


Fig. 4. Methanol production with various promoted tungsten oxide photocatalysts.

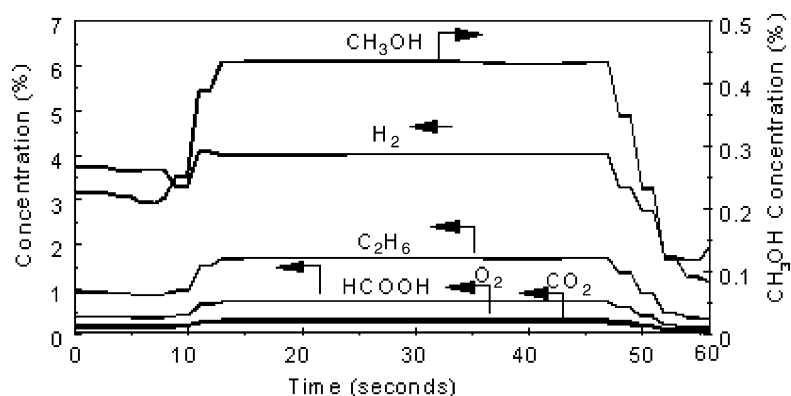


Fig. 5. Products of the photocatalytic conversion of methane in methane hydrate with lanthanum-promoted tungsten oxide photocatalyst.

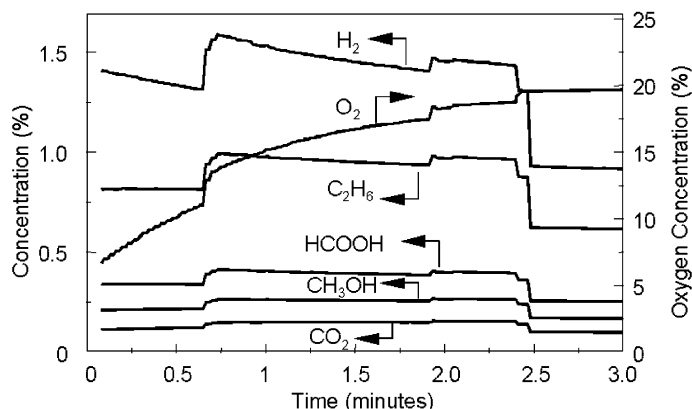


Fig. 6. Products of photocatalytic conversion of methane in methane hydrates with a sol-gel titanium dioxide photocatalyst.

illumination revealed the presence of methanol, hydrogen, ethane, oxygen, formic acid, and carbon dioxide. The formation of methanol and hydrogen are the primary products of reaction. The other products observed are formed by side reactions. Photocatalytic splitting of water (a side reaction not shown but observed in our laboratory when using this catalyst) forms oxygen. Ethane is formed by the combination of two methyl radicals (produced in Eq. (5)), and formic acid and carbon dioxide are the result of further reactions of methanol.

The results of photocatalytic conversion of methane contained within methane hydrates with a sol-gel titanium dioxide photocatalyst is shown in Fig. 6. Note that while methanol and hydrogen are produced by the reaction, oxygen is the main product.

#### 4. Conclusions

By use of a photocatalyst and electron-transfer reagent, we have been able to convert methane and water to methanol and hydrogen. Products of conversion at atmospheric pressure and 10.1 MPa were similar. While photoconversion of methane and water to methanol and hydrogen did not occur below 343 K at 1.0 MPa, conversion was observed at 323 K at 10.1 MPa and at temperatures as low as 258 K in methane hydrates. We also observe several side reactions of methane conversion in all instances, the production of ethane, oxygen, formic acid and carbon dioxide.

Under the conditions used in the 1 MPa experiments, the photocatalytic reaction produced 1.7 g

of methanol per gram of catalyst per hour in the steady-state mode and produced 43 g of methanol per gram of catalyst per hour when hydrogen peroxide solution was added.

The use of a filter removed the UV component from the lamp. Experimental results show that little difference between the filtered and unfiltered lamp was observed in the case of the platinum-doped tungsten oxide sample. This indicates that the photocatalyst is operating using visible light, the UV portion of the lamp's output is negligible in the photocatalytic conversion of methane to methanol, and that a limiting factor in conversion may be the solubility of methane in water.

In all experiments, conversion of methane and the production of methanol are augmented by the addition of hydrogen peroxide solution, consistent with the postulated mechanism that invokes a hydroxyl radical as an intermediate in the reaction sequence. The use of other radical initiators would be of interest to determine if the enhanced conversion could be sustained.

## 5. Disclaimer

Reference in this report to any specific commercial product, process, or service is to facilitate understanding and does not necessarily imply its endorsement or favoring by the United States Department of Energy.

## Acknowledgements

The author would like to acknowledge the technical assistance of Richard R. Anderson, John Baltrus, Bradley C. Bockrath, Joseph R. D'Este, J. Rodney Diehl, Heather A. Elsen, Elizabeth A. Frommell, Neil Johnson, Edward P. Ladner, Donald V. Martello, Richard P. Noceti, and Joseph P. Tamilia.

## References

- [1] K. Ogura, M. Kataoka, *J. Mol. Catal.* 43 (1988) 371.
- [2] K. Ogura, C.T. Migita, M. Fujita, *Ind. Eng. Chem. Res.* 27 (1988) 1387.
- [3] M. Ashokkumar, P. Maruthamuthu, *J. Mater. Sci. Lett.* 24 (1988) 2135.
- [4] P. Maruthamuthu, M. Ashokkumar, *Int. J. Hydrogen Energy* 14 (4) (1989) 275.
- [5] P. Maruthamuthu, M. Ashokkumar, K. Gurunathan, E. Subramanian, M.V.C. Sastri, *Int. J. Hydrogen Energy* 14 (8) (1989) 525.
- [6] R.P. Noceti, C.E. Taylor, J.R. D'Este, *Catal. Today* 33 (1997) 199.
- [7] R.P. Noceti, C.E. Taylor, J.R. D'Este, US Patent 5,720,858 (1998).
- [8] C.E. Taylor, R.P. Noceti, *Catal. Today* 55 (3) (2000) 259–267.
- [9] Adapted from V.A. Kuustraa, E.C. Hammershaimb, *Handbook of Gas Hydrate Properties and Occurrence*, US Department of Energy, DOE/MC/19239-1546, December 1983, p. 48.
- [10] C.E. Taylor, R.P. Noceti, B.C. Bockrath, US Patent 6,267,899 (July 31, 2001).
- [11] J.A. Dean (Ed.), *Lange's Handbook of Chemistry*, 13th ed., 1985, pp. 10–15.